Modeling of the Coronal Mass Ejection that Triggered the Third Largest Geomagnetic Storm of Solar Cycle 24

THE UNIVERSITY OF ALABAMA IN HUNTSVILLE

CENTER FOR SPACE PLASMA & AERONOMIC RESEARCH

Dinesha V. Hegde[1,2], Talwinder Singh[2], Tae K. Kim[2], Nikolai V. Pogorelov[1,2]

[1] Department of Space Science, The University of Alabama in Huntsville, Huntsville, AL 35899 USA

[2] Center for Space Plasma and Aeronomic Research (CSPAR), The University of Alabama in Huntsville, Huntsville, AL 35899 USA

DEPARTMENT OF SPACE SCIENCE
THE UNIVERSITY OF ALABAMA IN HUNTSVILLE

Introduction

- ★ Coronal mass ejections (CMEs) are powerful explosions of plasma and magnetic field that is released from the Sun's corona and travels through the interplanetary space that can have a significant impact on the interplanetary medium and our planet.
- ★ On August 26, 2018, during the declining phase of solar cycle 24, the third-strongest geomagnetic storm (Dst = -175nT) of the cycle occurred due to a CME that erupted from the Sun on August 20, 2018.
- ★ Remarkably, this particular event was caused by a slower and smaller CME, which is unusual as fast and large CMEs are typically responsible for geomagnetic storms. (e.g. Gopalswamy, 2018).
- ★ Previous studies (Gopalswamy et al.2022 and Chen et al. 2019) have reported that the flux rope associated with this CME had a complicated rotation in the interplanetary medium before it reached Earth, and the high-density structure in the magnetic cloud observed at Earth.
- ★ In this study, we employ a data-constrained constant-turn flux rope-based 3D Magnetohydrodynamic (MHD) model (Singh et al 2022) to simulate the propagation of this CME through a time-dependent, data-driven ambient solar wind (SW).
- ★ We utilize parameters from a graduated cylindrical shell model to constrain the flux rope model, which was obtained by fitting coronagraphic observations of the CME, including data from the Heliospheric Imager (HI) on STEREO-A.
- ★ Our research highlights the significance of MHD modeling CME propagation to gain a better understanding of the dynamics of these events and their impact on the Earth's space environment.

Methodology

❖ Solar Wind Model : HelioCubed

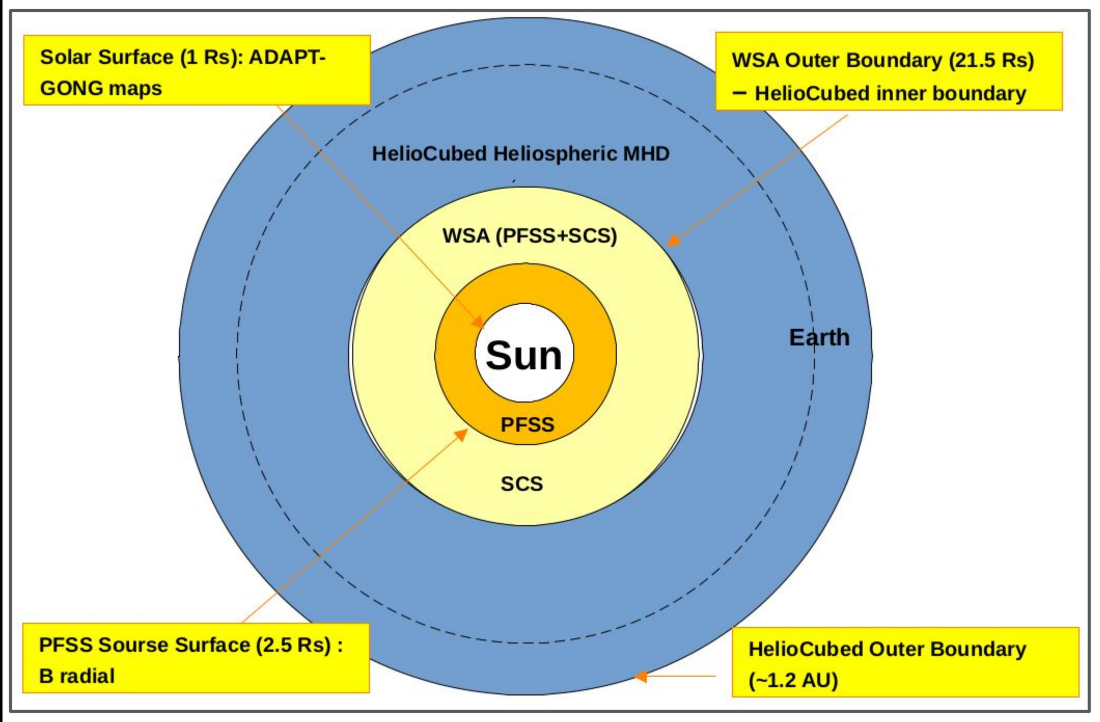

- ★ HelioCubed is a highly parallel, GPU enabled, adaptive mesh refinement (AMR) based solver for the hyperbolic, Reynolds-averaged, ideal MHD equations in conservative form.
- ★ Using the recently built Proto framework, It employs finite-volume method to solve MHD equations with fourth order of precision in space and time on cubed-sphere grids, which resolves the polar singularity intrinsic in the spherical grid.
- ★ Currently, we use the already implemented second order finite-volume MHD solver on a spherical grid to solve the Ideal MHD equations in the inner heliosphere.

Fig-1: (Left) Diagram showing the time-dependent inner-heliospheric solar wind model used in this study (not to scale).We use Air Force Data Assimilative Photospheric Flux Transport (ADAPT; Arge et al., 2013) driven Wang-Sheeley-Arge (WSA) coronal model (Arge et al, 2003, 2004), to derive boundary conditions for HelioCubed

❖ CME Model : FRiED + Constant-Turn Flux Rope

- ★ We use the geometry of the FRiED model (Isavnin 2016), which simplifies the CME shape to a croissant-like structure with two legs rooted at the center of the Sun, to simulate flux-rope-based CMEs.
- ★ To characterize the geometry of the CME, we use the Graduated Cylindrical Shell Model (GCS; Thernisien, 2011) since FRiED geometry can be derived from GCS (Singh et al, 2022)
- ★ To describe the initial magnetic field inside the flux rope, we use the uniform-twist flux rope model (Vandas & Romashets, 2017) analytic solution.
- ★ We insert this flux rope into the ambient SW in such a way that the flux rope is initially superimposed with the SW background. This superimposition is described in detail by Singh et al., 2020.
- ★ Further the model flux rope propagates through the inner heliosphere as an Interplanetary CME. (For more information see Singh et al, 2022)

References

- Arge, C. N., Henney, C. J., Hernandez, I. G., Toussaint, W. A., Koller, J., & Godinez, H. C. (2013), in AIP Conf. Series, Vol. 1539, Solar Wind 13, ed. G. P. Zank, et al., 11
- Arge, C. N., Luhmann, J. G., Odstrcil, D., Schrijver, C. J., & Li, Y. (2004), J. Atmosph & Sol-Ter Physics, 66, 1295
- Arge, C. N., Odstrcil, D., Pizzo, V. J., & Mayer, L. R. (2003), in AIP Conf. Proc. 679: Solar Wind Ten, 190
- Chen, C., Liu, Y. D., Wang, R., Zhao, X., Hu, H., & Zhu, B., 2019, ApJ, 884(1), 90.
- Gopalswamy, N., Yashiro, S., Akiyama, S., Xie, H., Mäkelä, P., Fok, M.-C., & Ferradas, C. P., 2022, JGR-SP, 8, 127.
- Isavnin, A. 2016, ApJ, 833, 267
- Singh, T., Kim, T. K., Pogorelov, N. V., & Arge, C. N. 2022, ApJ, 933, 2
- Vandas, M., & Romashets, E. 2017, A&A, 608, A118

Results

❖ GCS Reconstruction

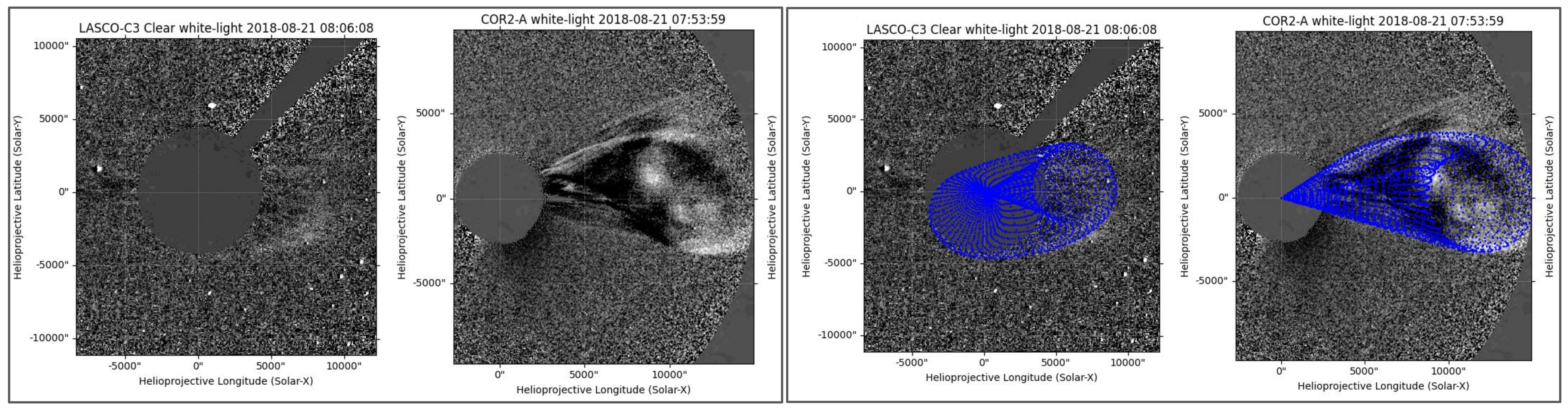

Fig-2 : (Left) Ambient solar wind radial velocity from HelioCubed at 2018 Aug 22, 06:09 UT (ecliptic plane) . (Right) CME inserted to the ambient solar wind as a constant-turn flux rope characterised based on the GCS model fit at the apex hight of the CME at 67.92 Rs (at 2018 Aug 22, 08:09 UT)

❖ CME Insertion & Propagation

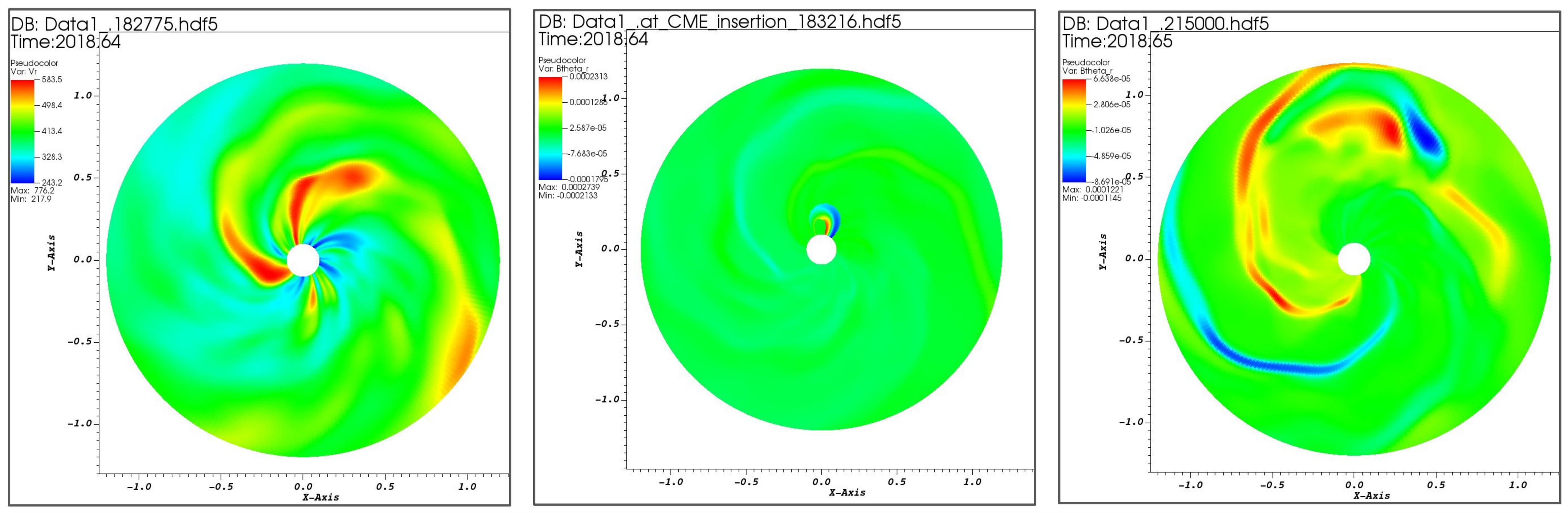

Fig-3 : (Left) Ambient solar wind radial velocity from HelioCubed at 2018 Aug 22, 06:09 UT (ecliptic plane) . (Middle) CME inserted to the ambient solar wind as a constant-turn flux rope characterised based on the GCS model fit at the apex height of the CME at 67.92 Rs (at 2018 Aug 22, 08:09 UT) B-theta Component. (Right) Evolved CME Fluxrope in the equatorial plane.

❖ CME Arrival at Earth

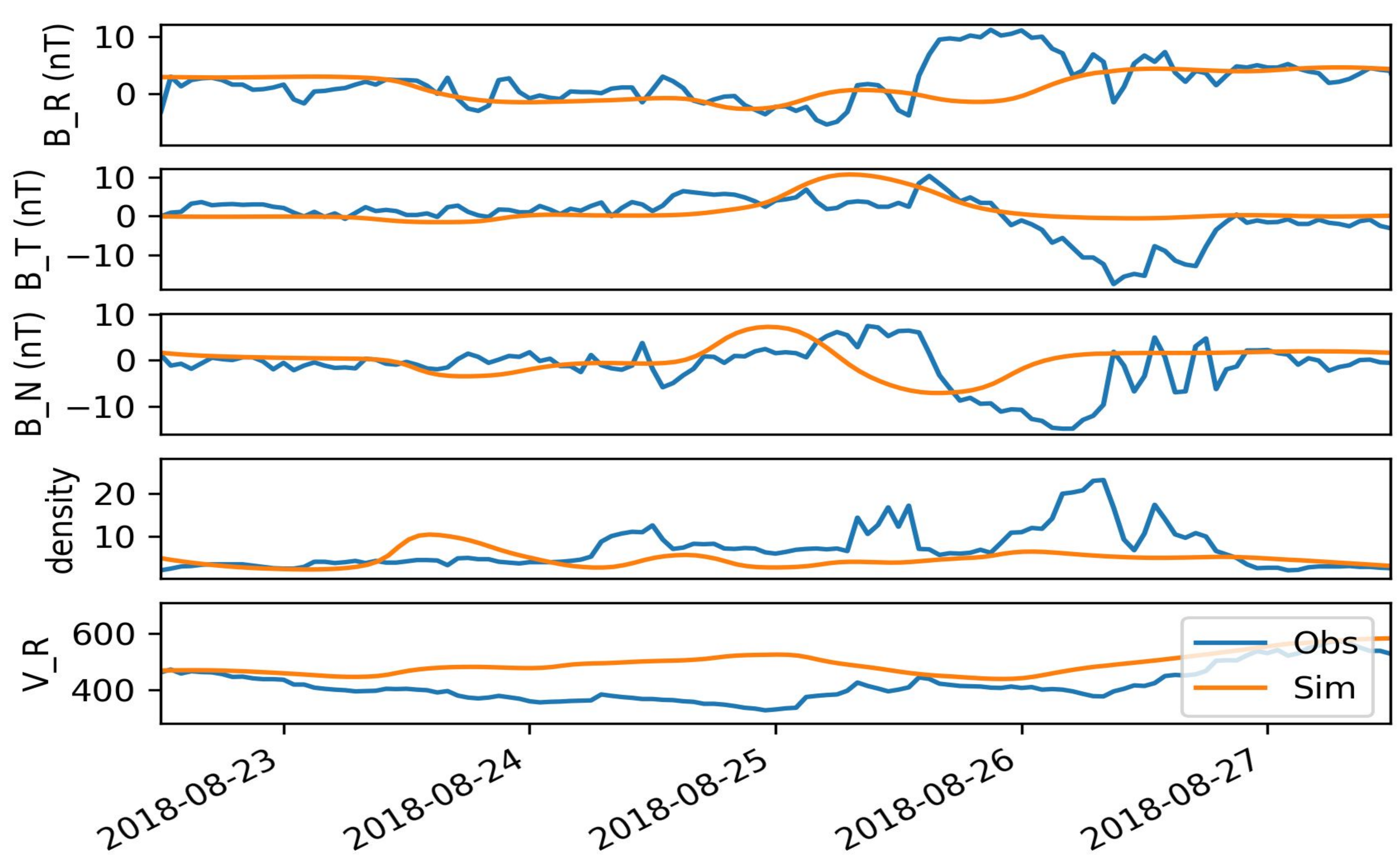

Fig-4 : Comparison of solar wind + CME simulation with the observation from OMNI database at Earth. Orange: Simulation and Blue : Observation. We will find the orientation of the flux rope using Marubashi flux rope fitting and inquire about the speculated complex rotation of the CME.

Acknowledgement

We acknowledge the use of data produced collaboratively between the Air Force Research Laboratory (AFRL) and the National Solar Observatory/GONG. The ADAPT model development is supported by AFRL. We also acknowledge the supercomputer time allocation from TACC Expanse and Stampede2 by NSF project MCA07S033. DVH acknowledges the support from the NASA FINESST grant 80NSSC22K0058. NP and TS was supported, in part, by NSF/NASA Space Weather with Quantified Uncertainty (SWQU) grant 2028154.